



Murdoch
UNIVERSITY

MURDOCH RESEARCH REPOSITORY

This is the author's final version of the work, as accepted for publication following peer review but without the publisher's layout or pagination.

Whale, J. (1993) *Application of particle image velocimetry to wind turbine wakes*. In: Proceedings of SPIE - The International Society for Optical Engineering. Volume 2052, 1993, pp. 667-674.

<http://researchrepository.murdoch.edu.au/12956/>

It is posted here for your personal use. No further distribution is permitted.

The Application of Particle Image Velocimetry to Wind Turbine Wakes.

Whale, J. and Anderson, C.G.

Fluid Dynamics Unit
Department of Physics
University of Edinburgh

Abstract

Wind turbine performance is critically dependent on the geometry of the rotor wake. Acquisition of detailed wake data is of major importance for further development of wind turbine studies.

This paper presents the results of a preliminary experimental study of the flow past a model turbine using Particle Image Velocimetry (PIV), a whole field velocimetry method, with a scanning beam system of flow illumination. The results strongly validate the PIV technique applied to studying wind turbine wakes. PIV provides the means whereby detailed full-field data can be obtained and an experimental data base for wake velocities and structure established.

1 INTRODUCTION

The need to understand the structure of the wake shed behind wind turbine rotors stems from two factors. Firstly, wind turbine performance is critically dependent on the geometry of the rotor wake. The wake structure determines the rotor inflow conditions and hence the forces on the blades. For design purposes it is essential to predict the blade loads accurately, to estimate rotor power output and structural stress. Thus, an accurate prediction of the wake structure is a dominant factor for reliable wind turbine aerodynamic prediction codes. Secondly, the turbulent downstream flow in wind turbine arrays is a limiting factor in terms of machine spacing. Better information on wake structure will allow optimum array spacing.

However, the lack of detailed experimental data in the wake of a turbine, and the difficulty of obtaining it, is widely appreciated. Full-scale visualisation experiments are difficult to perform and are limited by the problems of expense and non-repeatable conditions. Thus, though the investigations of wind turbine wakes are comparatively recent, many have involved simulators and model wind turbine generators. A good literature review is given by Luken[1]. In the late 1970s, wind tunnel simulations began in Holland (at TNO Apeldoorn), Sweden (Aeronautical Research Institute) and in the UK (at CERL Leatherhead). The work was co-ordinated by the International Energy Agency (IEA) and concentrated on hot-wire measurements of flow over tipvane type simulators. A summary of the experimental results for models of size 200-300mm in diameter can be found in Vermuelen[2]. Green[3] later refined and developed the modelling techniques using laser doppler anemometry (LDA) on a modified model aircraft propeller of diameter 150mm.

The problems of poor signal to noise ratio and condensation of seeding in the wind tunnels experienced by LDA workers ([4], [5]) together with the desire to obtain simultaneous multipoint measurements with minimum disturbance to the flow caused by instrumentation, suggest the method of Particle Image Velocimetry (PIV) to studying flows of this type.

PIV is a non-intrusive velocity measurement technique which allows complete two-dimensional flow fields to be captured at a single instant. The basis of PIV is to stroboscopically illuminate a two-dimensional plane of flow containing small neutrally buoyant seeding particles by means of a sheet of pulsed light. A double (or multiple) exposure photograph of this plane is taken. The spacing between the images of each particle on the film gives the local velocity. This photograph is then analysed over a grid of points to determine the local flow velocities across the whole field.

The technique of PIV was introduced to the field of wind turbine aerodynamics by Smith et al.[6] who conducted tests on a Rutland wind turbine using pulsed lasers. The tests established the applicability and usefulness of the PIV technique as a velocimetry tool for wind turbines. However, the high slipstream velocities involved in wind tunnel testing meant that particles

separating at the trailing edge of the blades were dispersed out of the light sheet causing problems of illuminating the wake structure. This limited the study to flow close to the blade and again illustrated the problems of seeding in wind tunnels.

In an attempt to overcome the problems of illumination and seeding density experienced by previous investigators in wind tunnel studies, some preliminary tests of a model turbine rig in water were conducted in the Fluid Dynamics Unit of the University of Edinburgh starting in December 1991. The PIV experiments were performed using a high powered continuous wave (CW) laser with the turbine placed in a water tank capable of generating currents. The blade passing frequency of the rotor and the upstream current were carefully arranged so that, Reynolds number apart, aerodynamic similarity existed between the model and a full-scale wind turbine.

The results of those experiments and the conclusions to be drawn from them are presented in this paper.

2 EXPERIMENTS

The experiments were carried out in a glass-based, two-dimensional wave flume which is 10m long, 0.4m wide and a filled with water up to a depth of 0.75m. The tank was equipped with a recirculating pump which allows a steady flow velocity to be established. The model turbine rig was placed across the tank subjecting the rotor to a uniform current. The turbine was driven by a 14W electric motor/generator suspended on a frame above the water level. The rotor is located at the end of an inverted tube, which also acts as a shroud for a toothed drive belt connected to the motor. The inverted pipe, or tower, is perpendicular to the oncoming flow to ensure symmetric inflow conditions (See Figure 1.)

It is important that the mechanism of wake generation is accurately produced. As well as geometric similarity between the model and a full-scale machine, an appropriate range of tip speed ratios λ are used (ratio of blade rotation to freestream velocity) so that, notwithstanding the Reynolds number, kinematic similarity is assured. Motor speed was altered to achieve the desired tip speed ratios

$$\lambda = \frac{\omega R}{V_0},$$

where R is the radius of the rotor, ω is the blade passing frequency and V_0 is the freestream velocity. Blade rotation was measured from the output voltage reading of the tachogenerator while the average upstream current was initially estimated from valve settings of the recirculating pump and then, more accurately, derived from PIV analysis.

The PIV set-up at Edinburgh is based on the scanning beam system of flow illumination[7]. The beam from the 15W CW Argon ion laser is narrowed, collimated and reflected from an octagonal rotating mirror onto a parabolic recollimating dish. This is positioned beneath the centre of the flume and directs the beam vertically upwards through the glass base of the wave tank. As the octagonal mirror rotates, the laser beam scans over the parabolic mirror and the beam sweeps through the area of interest, illuminating a vertical cross-section of the flow field. The water was seeded with conifer pollen of average diameter $70\mu\text{m}$ with concentrations maintained at a level to ensure a high density of non-overlapping particles on the resulting film record.

Two types of rotors were used in the experiments. In the preliminary investigations the turbine was a 2-blade model aeroplane propeller of 175mm diameter and 16mm in chord length at a blade span of 70%. The propeller was run in reverse so that its twist and chord distributions approximated those of a wind turbine rotor. The flowrate was set to an estimated 250mm/s, the laser power to 9W and the illumination interval to 8.02ms. Tip speed ratios of approximately 3-12 were used with Reynolds number based on tip chord in the range 6,000 - 35,000. Photographs of the flow were taken with a standard 35mm Nikon FM2 camera with motor film advance and a f2.8 50mm flat focus lens (e.g. Figure 2). 24 exposures are made on 400 ASA film including one of a calibration grid from which an Image/Object magnification, $M = 0.05$, was obtained after developing the film.

The second set of experiments involved some improvements in generating a more realistic wind turbine simulator and enhancing the quality of the measurement data. The propeller was not an ideal turbine model as its aerofoil section operated trailing edge first so it was replaced by flat-plate blades of the same diameter with varying thickness, camber and taper. The tower of the rig was streamlined with a foam plastic shroud in order to limit its wake interfering with the top half of the turbine wake structure, as was noticeable in early tests. A wide range of velocities were recorded in the previous experiments, from the undisturbed upstream flow to the region of almost stagnant fluid behind the rotor. Thus, for these experiments, an image shifting system was used to impose a translational velocity on the recorded image to increase dynamic range and eliminate directional ambiguity. The shift system was comprised of a Hasselblad 500 EL/M camera and 80mm lens mounted on a turntable and controlled by a microcomputer which rotated the turntable to a given shift speed and triggered the camera when it reached the correct position. A shift speed of 30rad/s was used to impose a translational velocity on the flow in the opposite direction to the 200mm/s freestream and the camera position chosen so as to optimise the dynamic range, ΔV . Given the magnification, $M = 0.0958$, an illumination interval of $T = 4.00\text{ms}$ was chosen to capture maximum analyzable particle displacements, Δd , on the film according to the relation

$$\Delta d = M\Delta VT$$

The PIV negatives were analysed on a 32 bit microcomputer to yield 2D velocity vector maps. The film was interpreted point by point over a dense grid using methods of optical and digital analysis. This involves scanning a small part of the negative at a time with a probe laser to produce an interference pattern from the multiple particle images in that area. The interference fringes are measured and recorded in digital form and the data Fourier transformed to yield the particle velocities at that point. The whole negative is scanned in this way to build up a flow velocity map, which forms the basis of all subsequent analysis. Firstly the shift velocity has been subtracted at all points to reveal the actual flow pattern and then the mean horizontal component of the velocity has also been subtracted in order to highlight the induced flow velocities. The velocity information can also be processed to produce vorticity maps. The contours of the plots join points of equal vorticity with vortex strengths represented by varying degrees of lightness.

3 RESULTS

3.1 EXPECTATION FROM THEORY

A study of the aerodynamics of the flow around the rotor blade allows insight into the expected structure of the wake behind a wind turbine.

The net imbalance of the pressure distribution around a blade is the physical mechanism for generating lift on the blade. As a by-product of this mechanism the flow near the blade tips tends to curl around the tips as it is forced from the high pressure region on the bottom surface of the blade to the high pressure region on the top surface. There is a discontinuity in the tangential velocity at the trailing edge of the blade since the streamlines leaving the trailing edge from the top and bottom surfaces are in different directions. The large velocity gradients at the trailing edge generate a thin region of shear flow with very large vorticity. Thus a continuous vortex sheet is shed downstream from the trailing edge. The combination of rotating blades and an oncoming flow form a helical vortex system as the sheet becomes a screw surface. However the stability of the sheet is dependent on the velocities normal to the sheet induced by the vortex elements that the sheet is comprised of. These self-induced distortions deform the wake as the sheet "rolls up" forming regions of concentrated vorticity. The induced velocities are proportional to the spanwise rate of change of circulation around the blade. Thus the sheet tends to roll up at the edges and helps to form blade-tip vortices. Hence the helical vortex system becomes a spiral path of trailing vortices. In the flow recording process, the PIV illumination extracts behaviour in the wake corresponding to a cross-section of the helical vortex system.

3.2 ANALYSIS

The development of the turbine wake depends on the various rotor states as defined in Eggleston and Stoddard[8]. At low tip speed ratios, the rotor is in the windmill state. The wake of the turbine contains an area of expanding flow with reduced velocity. This is verified by the PIV velocity map of the propeller at $\lambda = 2.7$ (Figure 3) in that the velocity vectors in the wake point upstream after subtracting the mean horizontal velocity. In the lower half of the wake, angled strips of vorticity can be clearly seen; the expected pattern for the cross-section of a helical vortex sheet. Also seen from the velocity map is a sinusoidal pattern imposed on the boundary of the wake. This is consistent with the presence of trailing tip vortices originating from the rotating blades and passing downstream.

Figure 4 displays the corresponding vorticity map of Figure 3. Note how the wake is roughly divided into regions of positive(light) and negative(dark) vorticity, lying on either side of the centreline. This is again as expected from the cross-section of a helical vortex. The appearance of two sets of trailing vortices in each half of the wake can be explained from the design of the model propeller which has a rapid change in chord and twist near the hub as well as a change in chord near the tip. The subsequent rate of change of circulation around these parts of the blade induces velocities which roll up the vortex sheet both at the tip and at the hub.

As the tip ratio is increased, the rotor becomes more of a blockage to the flow. The wake becomes turbulent preserving the energy within the trailing vortices and producing a very strong vortex pattern. Figure 5 is a PIV velocity vector map for a flat-plate blade at a high tip speed ratio ($\lambda = 9.0$). The flat-plate had a thickness of 1.26mm, a camber of 6% and a linear taper with a chord length of 83% of the hub chord at the 70% span position. The presence of recirculating flow can be seen from the vector map indicating that the rotor is in the turbulent wake state. This is further substantiated by the vorticity contour map of Figure 6 as the boundary of the wake is characterized by initial expansion followed by marked contraction.

The limiting behaviour of the above state occurs at very high tip speed ratios when the recirculating vortices expand and move upstream to just behind the rotor plane. The laser sheet then illuminates a cross-section of a toroidal vortex and the rotor is in the so-called vortex ring state. It is not an operating regime commonly experienced by a real wind turbine.

Comparing the results from the preliminary experiments with the propeller and the later experiments with the flat-plate blades, the streamlining of the tower proved effective in reducing the interference with the top half of the wake and produced a more symmetrical flow pattern. The image-shifting succeeded in resolving the very small velocities in the almost stagnant region of flow behind the rotor at the analysis stage and eliminating problems of vector direction at the editing stage. Also, the large format film was justified in capturing a global view of the wake structure and giving a better indication of the bulk flow.

4 CONCLUSIONS

The models clearly exhibited operating states characteristic of a wind turbine, namely the windmill state and the turbulent wake state. The windmill state is the intended state for wind turbine operation. The energy is extracted from the wind and converted to shaft power while the wind is slowed accordingly. However, turbulent wake states do occur during operation and much modelling needs to be done to have a complete understanding of the forces and moments on a rotor in this state.

Care must be taken when comparing the performance of a model wind turbine to that of a full scale machine. As pointed out by Galbraith et al.[9], interpretation of turbine performance requires reliable data on the characteristics of the aerofoil at the appropriate Reynolds number; the overall properties of the downstream wake, however, are less sensitive to Reynolds number and inferences can be made from bulk-flow phenomena.

The results strongly justify using the PIV technique to study flows of this type. PIV provides the means whereby detailed full-field data can be obtained and an experimental data base for wake velocities and structure established. The amount of high quality detailed data of the

entire flow field obtained by the uncomplicated, quick and flexible approach of PIV compared favourably with the previous methods explored by investigators. The potential for this method is significant and can be used to compare wake data from other experiments as well as wake geometries predicted by numerical codes. In particular, it could provide information about those regions of flow where theoretical techniques give least satisfactory results, for example in stalled flows. This is a question of some importance to the wind turbine industry as current design methods for stall-regulated wind turbines are essentially empirical.

5 ACKNOWLEDGEMENTS

The authors sincerely wish to thank Dr. D. Skyner and Mr. T. Bruce for their advice and assistance on matters relating to PIV and Dr. M.L. Jacobsen for assistance with laser beam alignment. Funding for this work was supplied by the Hackett Studentship of the University of Western Australia with additional financial support provided by the Overseas Research Award Scheme.

References

- [1] E. Luken. Literature data-base on wind turbine wakes and wake effects. *MT-TNO Report 86-351 (IEA -9-NL04) Apeldoorn, Holland.*, 1986.
- [2] P.E.J. Vermeulen. Studies of the wake structure of model wind turbine generators. *TNO Report 79-012904 Apeldoorn, Holland*, 1979.
- [3] D.R.R. Green. Modelling large wind turbines and wakes. *PhD Thesis, Loughborough University*, 1985.
- [4] M.B. Anderson, D.J. Milborrow, and J.N.. Ross. Performance and wake measurements on a 3m diameter hawt : comparison of theory, wind tunnel and field test data. laser doppler anemometry. *ETSU contract E/5A/CON/1090/177/020 Cavendish*, 1982.
- [5] J.N. Ross and J.F. Ainslie. Wake measurements in clusters of wind turbines using laser doppler anemometry. *Proceedings of the 3rd British Wind Energy Conference, Cranfield*, 1981.
- [6] G.H. Smith, I. Grant, A. Liu, and D.G. Infield. Diagnostics of wind turbine aerodynamics by particle image velocimetry. *Proceedings of the 12th British Wind Energy Conference, Norwich*, 1990.
- [7] C. Gray, C.A. Greated, D.R. McCluskey, and W.J. Easson. An analysis of the scanning beam piv illumination system. *J.Phys :Measurement Science and Technology*, 2:717-24, 1991.
- [8] D.M. Eggleston and F.S. Stoddard. *Wind Turbine Engineering Design*. Van Nostrand Reinhold, New York, 1987.
- [9] R.A.McD. Galbraith, F.N. Coton, E. Saliveros, and G. Kokkodis. Aerofoil scale effects and the relevance to wind turbines. *Proceedings of the 9th British Wind Energy Conference, Edinburgh*, 1987.

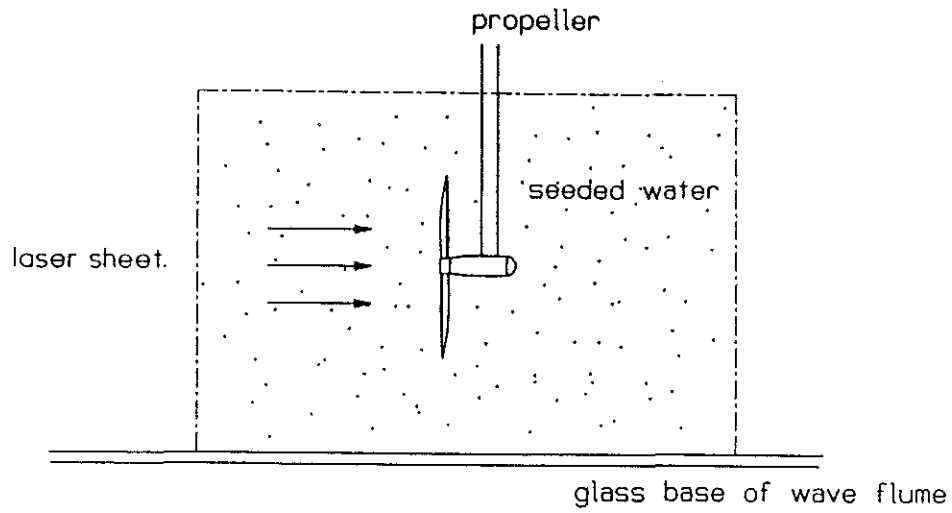


Figure 1. Schematic diagram of PIV recording process.

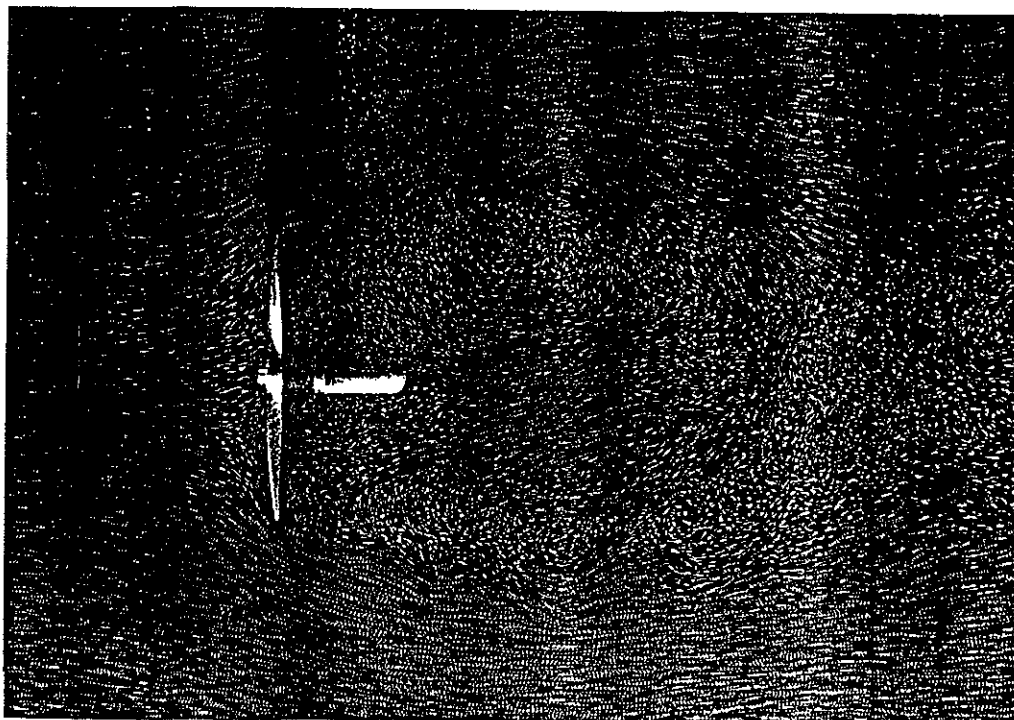


Figure 2. Photographic PIV record of flow past propeller.

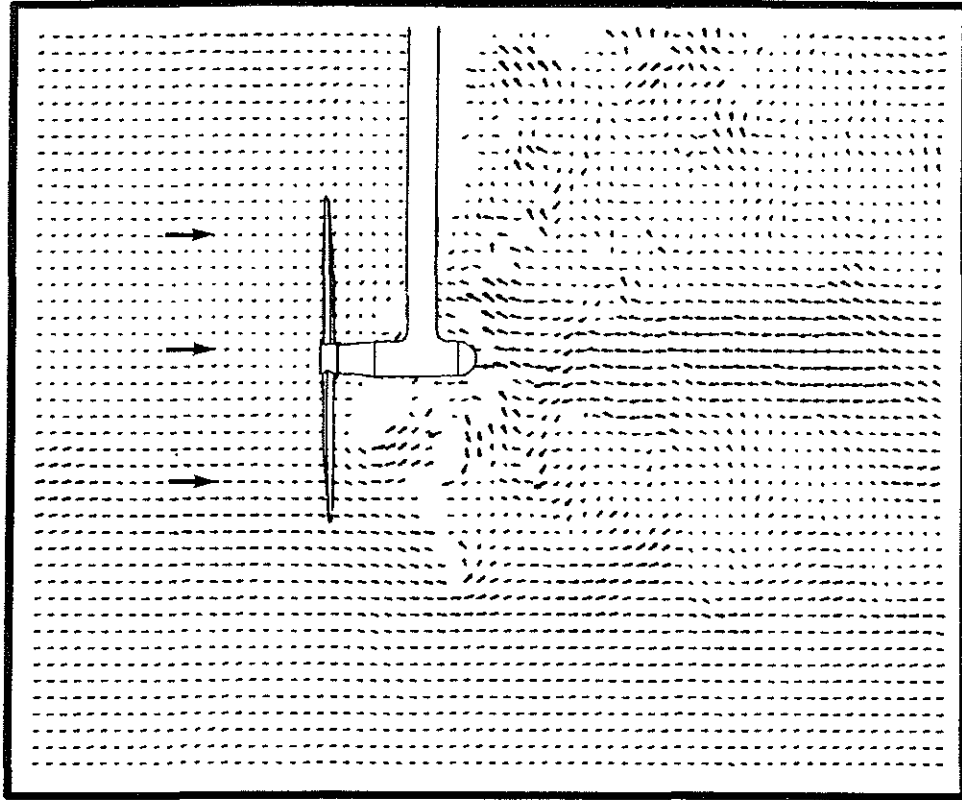


Figure 3. PIV velocity vector map of propeller in windmill state ($V_0 = 250\text{mm/s}$, $M = 0.050$, $T = 8.02\text{ms}$).

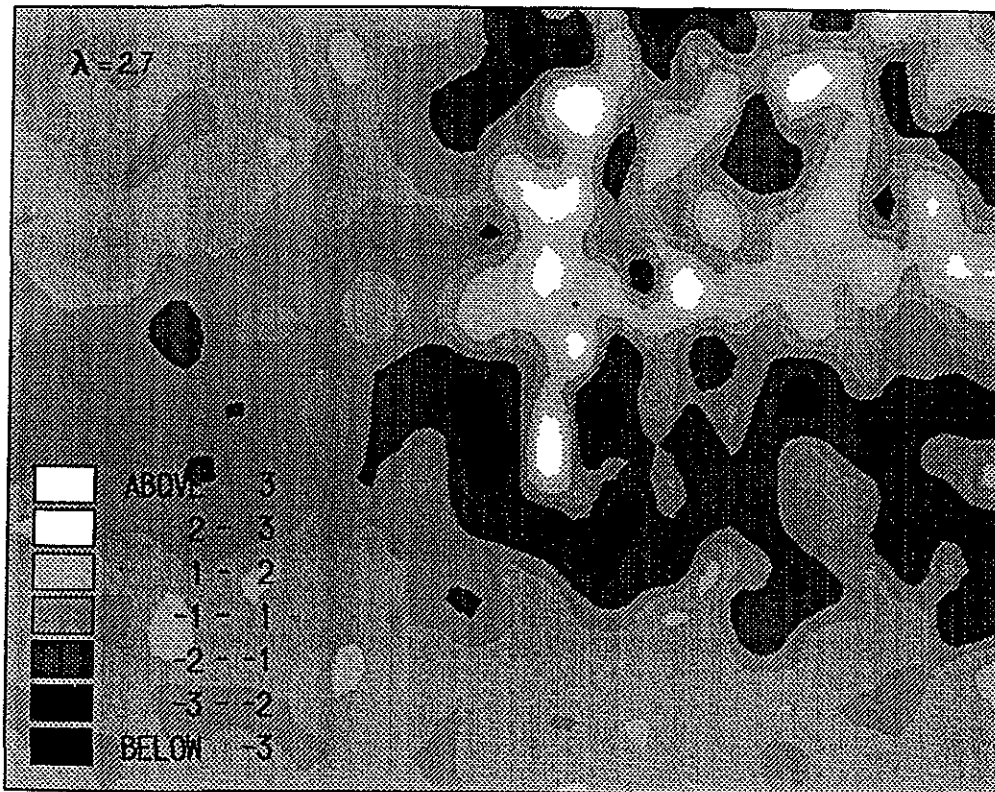


Figure 4. PIV vorticity map corresponding to Figure 3.

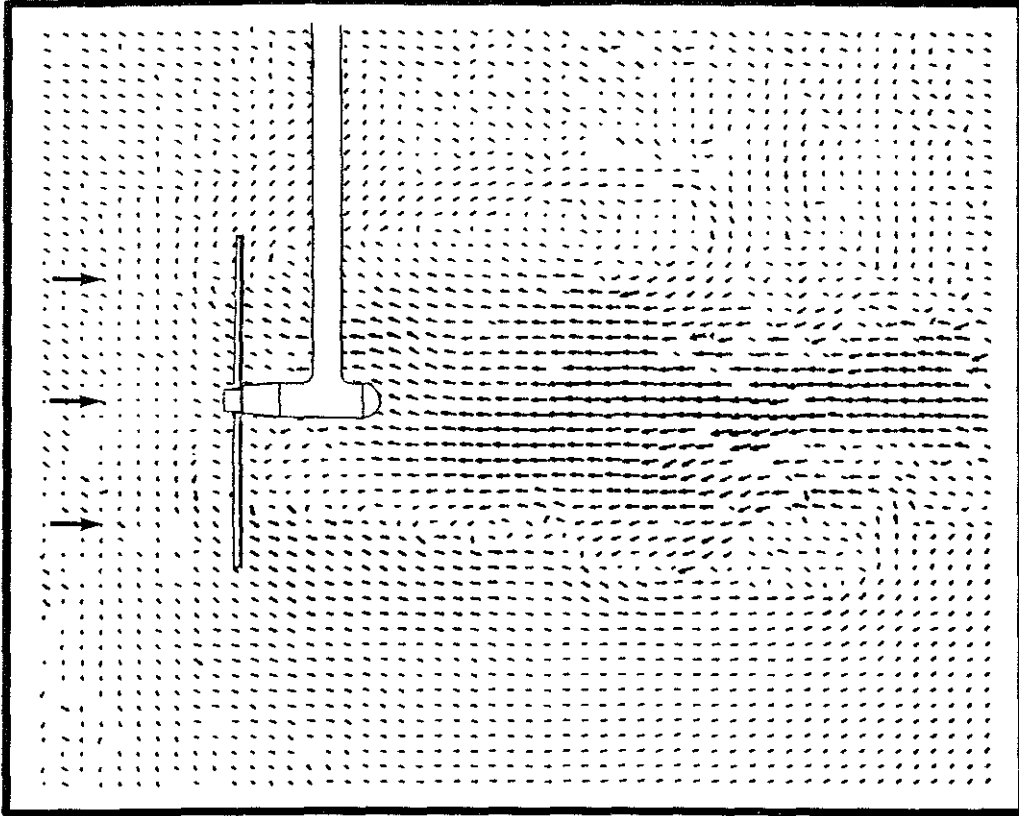


Figure 5. PIV velocity vector map of flat-plate blade in turbulent wake state ($V_0 = 200\text{mm/s}$, $M = 0.096$, $T = 4.00\text{ms}$).

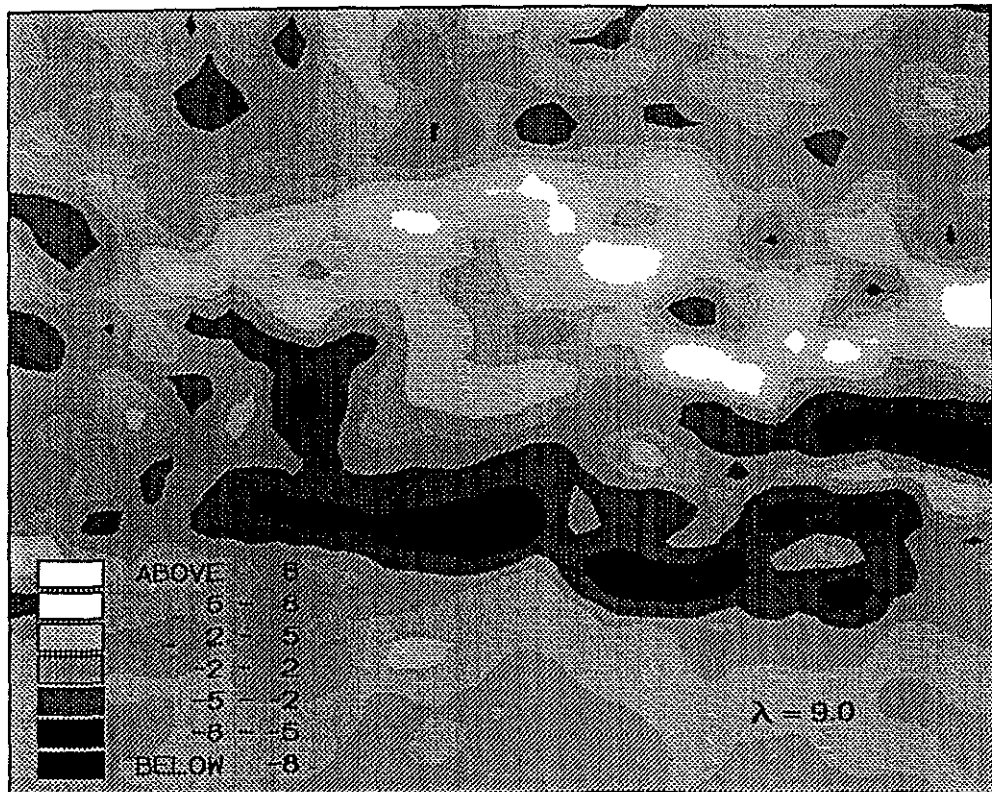


Figure 6. PIV vorticity map corresponding to Figure 5.